ENGINEERING RESEARCH INSTITUTE
THE UNIVERSITY OF MICHIGAN
ANN ARBOR

Final Report

S5W END-PLATE STRESS STUDY

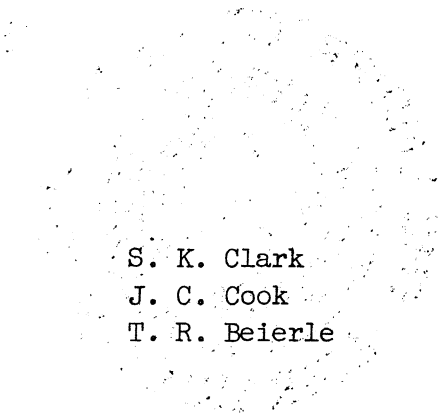

S. K. Clark
J. C. Cook
T. R. Beierle

Project 2658

WESTINGHOUSE ELECTRIC CORPORATION
PITTSBURGH, PENNSYLVANIA

August 1957

TABLE OF CONTENTS

ABSTRACT

Structural tests of the bottom-plate assembly of the Westinghouse S5W reactor were carried out using stress-coat and resistance strain gauges. Quantitative results are presented, using structural modeling laws to apply data from the models tested to the actual reactor barrel.

OBJECTIVE

This series of tests was designed to supplement and, where possible, to confirm the results of an analytical stress analysis on the bottom (end) plate of the Westinghouse S5W reactor shell. Strains were to be measured on models of the structure at points which appeared to be critical, based on the analysis, as well as at other selected points. Strain measurement was to be by both stress-coat and electric resistance strain gauges. Loadings were to be those considered in the analysis, namely, longitudinal loads on the modules, axial loads on the modules, and pressure on the entire structure. Reference should be made to Westinghouse drawing 513F412 for detailed shell dimensions. Additional information is contained in Ref. 2.

SUMMARY OF RESULTS

1. The largest values of stresses measured in the model and applied to the prototype occur during transverse loading at or near the junction of the first pass through tubes and the bottom plate. These are presented in Table IV.

2. Stresses arising from the dead weight of all modules acting on the structure are all very small compared with the allowable stresses.

3. Stresses due to 30-psi or 50-psi internal pressure are all below allowable limits. Experiments indicate that at 150-psi internal pressure certain regions will exceed allowable stresses.

4. In general, all gauges read strains which are linearly proportional to load on the model so that good linearity of the structure, such as exists, indicates that the model-prototype laws are applicable with small error here.

5. Some success in correlation of experiment with theory was obtained on those portions of the structure which are relatively clean and simple, such as the toroidal shell. Correlation is poor in regions of very complex structure, as might be anticipated.

PROCEDURE

Half-size models of the bottom plate of the S5W reactor shell were constructed of both aluminum and plexiglass, for purposes of structural testing. Three types of tests were performed: first, that in which the modules are loaded transversely (simulating a sideward shock); second, that in which the shell is subjected to an internal pressure; and third, that in which the shell is subjected to vertically axial loads, simulating the dead weight of the modules. A detailed description of the testing techniques and procedures follows.

A. INTERNAL PRESSURE TEST

Three possible internal pressure conditions exist for the prototype shell, namely, internal pressures of 30, 50, and 150 psi. Since the law re-

lating model stresses and pressures to prototype stresses and pressures is

$$\left(\frac{\sigma_m}{p_m}\right) = \left(\frac{\sigma_p}{p_p}\right) , \tag{1}$$

where

σ_m = model stress,
σ_p = prototype stress,
p_m = model pressure, and
p_p = prototype pressure,

then proper stresses will be read directly from the model at pressures corresponding to the prototype pressures, or alternatively,

$$\sigma_p = \left(\frac{p_p}{p_m}\right)\sigma_m , \tag{1a}$$

when one desires to use model pressures differing from those in the prototype. In this case air pressures of 50, 40, 30, and 20 in. of mercury were used as internal pressure in the model, and the prototype stresses were computed by first determining the model stresses from the appropriate strain-gauge data and then treating these by Eq. (1a) to obtain stresses existing in the prototype shell. These stresses in the prototype are presented in Table I for the three conditions of prototype internal pressure previously listed, namely, 30, 50, and 150 psi. The method of treating the raw strain-gauge data to obtain stresses in the model is given in the section of this report titled "Instrumentation," since it is common to all types of tests.

Pressures used in the model shell were restricted to 50 in. of mercury or less for safety reasons, since considerable energy was stored in the shell in the form of compressed air at these pressures. Pressure loading by water or oil was not thought feasible due to the necessity of thorough protection of the strain gauges. Rubber plugs were used to fill the first-pass stub-tube holes during this test. Figures 1, 2, 3, and 4 show views of the experiment after the readings had been taken.

During this test, a zero-pressure strain reading would be taken on a particular gauge, after which pressure would be slowly increased and strain read at 20, 30, 40, and 50 in. of mercury. These net strain readings were then all corrected to 30-psi internal pressure, assuming linearity, and an average value taken of the four results. In this manner zero drift was not a serious factor since the time involved was approximately 5 min, and by this averaging process very close reproducibility of results was obtained.

In chronological order of completion, the next test was that of loading the plexiglass model after stress-coat had been applied to it, the loading

being the same as the loading in the transverse or shock-load type of test. For this purpose a concrete block foundation was constructed and the plexiglass shell assembled into the wooden loading frame furnished by Westinghouse. Next the steel tubes simulating the modules were inserted and were loaded with rods and turnbuckles in such a fashion that equal reactions were felt by all stub tubes at the shell structure. Loads in each rod were monitored by inserting in each loading rod a ring dynamometer made of brass tubing which had two strain gauges attached at its midpoints and which had been previously calibrated. This arrangement is shown in Figs. 5 and 6.

The plexiglass shell was sprayed with the proper grade of stress-coat and loads sufficient to cause stub-tube reactions of 60 lb at the shell were applied. At this point cracks clear enough to photograph were noted. The cracks are shown in Fig. 7; the loads are directed downward. Sensitization was accomplished by spraying CO_2 onto the model, after which the pictures of Figs. 8 and 9 were taken. These show further cracking around the first-pass stub-tube holes and also around the upper edge of the toroidal shell itself. A complete sketch of the stress-coat crack pattern was made by hand (Fig. 10), which indicates the pattern after sensitization.

Based on the results of the stress-coat test of the plexiglass model, 10 more strain gauges were added to the aluminum model in places where early stress-coat cracking appeared, and these gauges were oriented in a direction perpendicular to the crack direction, thus attempting to obtain the direction of maximum strain. These gauges are numbered 106 through 115 on the coded drawing previously transmitted to Westinghouse.

B. TRANSVERSE LOADING TEST

The aluminum model was next mounted in the wooden frame and the whole assembly placed in the bed of a Baldwin-Southwark, 60,000-lb-capacity, hydraulic testing machine. Since it was not possible to load all of the steel tubes simulating modules at once, they were loaded two at a time in such a fashion as to produce a stub-tube reaction at the shell of 500 lb each. Tubes were loaded in pairs one after the other, and finally the sum of all strains read was taken to represent the effect of loading all tubes simultaneously. This technique presupposes linearity of the structure, which is almost certainly true. Again, zero drift of the gauges was held to a minimum by reading one gauge at a time while loading was taking place, and again reproducibility was excellent. Figures 11 and 12 show this test in progress. The net prototype stresses are computed on the basis of the equation

$$\sigma_p = \sigma_m \cdot \frac{L_p}{L_m} \cdot \frac{a_m^2}{a_p^2} , \qquad (2)$$

where

L_m = load on model, lb,
L_p = load on prototype, lb,
a_m = scale of model, and
a_p = scale of prototype,

which equation again presupposes linearity of the structure. The results of the strain-gauge readings on this test were converted to model stresses, which were in turn treated by Eq. (2), and the resulting prototype stresses are reported in Table II.

C. AXIAL LOADING TEST

The axial loading test was performed to determine the effect on stresses in the prototype of allowing the dead weight of the modules to rest on the stub tubes or on the area of the stub-tube spacer plate immediately adjacent to the stub tubes. For this, 18 legs were manufactured which could be bolted to the flange of the aluminum model. This model was then placed in a horizontal position on the bed of a 120,000-lb-capacity Riehle screw-type testing machine, and loads applied axially by means of loading two symmetrically located stub-tube holes using two plugs and a bridging cross beam. This test is illustrated in Figs. 13 and 14. Again, superposition with its implicit assumption of linearity was necessary since it was only possible to load two stub tubes at a time, and the strains resulting from these several loadings had to be summed to obtain the resultant strain at any gauge location for simultaneous axial loading of all stub tubes. Aside from changes in mechanical aspects of this test, the techniques used were identical to those used for the previous tests, except that the magnitude of the axial load reaction at each stub tube on the stub-tube radial spacer plate was set at 1000 lb.

INSTRUMENTATION

As previously stated, instrumentation during this test was primarily by means of wire-resistance strain gauges. In those places where space permitted, rosettes of type AR-1 were installed, but for the most part gauges of type A-18 were used. In many cases it was found possible to install these gauges in right-angled pairs, and these were helpful in determining maximum shear stresses by assuming that these right-angled pairs were oriented in the directions of principal strain. The remainder of the gauges were single. In all, 105 gauges were installed by Westinghouse and 10 by The University of Michigan, making a total of 115 strain readings for each loading condition.

The gauge leads were installed here after receipt of the model from Westinghouse. A single common side was wired to each gauge, while separate leads from the other leg of each gauge ran to a bank of multiposition switch

boxes. A battery-operated Baldwin-Southwark Type L strain-gauge bridge was used to read strain. Three or four gauges became inoperative due to shorting or broken grid wires during the test, but these were simply cut out of the circuit when the short could not be located.

The strain data from the rosettes were reduced in the conventional manner, such as is given by Hetényi.[1] The radius of the largest Mohr's stress circle was determined for stresses in the model from the strain-gauge data, assumming that stresses through the shell thickness are zero, and this maximum shearing stress was then treated by Eqs. (1), (1a), or (2) as applicable, to obtain stresses in the model.

For the gauges occurring in right-angled pairs, it was assumed in all cases that these pairs were oriented in the directions of maximum and minimum principal strain. Taking this as a starting point, Hooke's law for a biaxial stress field (assuming that σ_z, the stress component perpendicular to the thickness of the shell is zero) may be written

$$\begin{aligned} e_x &= \frac{1}{E}(\sigma_x - \mu\sigma_y) \\ e_y &= \frac{1}{E}(\sigma_y - \mu\sigma_x) \quad , \end{aligned} \tag{3}$$

and from these one may find the associated stresses

$$\begin{aligned} \sigma_x &= \frac{E}{1-\mu^2}(e_x + \mu e_y) \\ \sigma_y &= \frac{E}{1-\mu^2}(e_y + \mu e_x) \\ \sigma_z &= 0 \quad . \end{aligned} \tag{4}$$

Three possible Mohr's stress circles now exist. These have radii representing the maximum shear stress as follows:

(a) x-y plane

$$\tau_{max} = \frac{E}{2(1+\mu)}(e_x - e_y)$$

(b) x-z plane

$$\tau_{max} = \frac{E}{2(1-\mu^2)}(e_x + \mu e_y)$$

(c) y-z plane

$$\tau_{max} = \frac{E}{2(1-\mu^2)} (e_y + \mu e_x)$$

Using 10×10^6 as the modulus of the aluminum model, each of the above maximum shear stresses was computed for each pair of perpendicularly oriented gauges for each loading. For a particular loading, only the largest shear stress as found above was reported as the maximum shear stress.

Every effort was made to orient single gauges in the direction of maximum principal strain, but since the structure was very complex, no assurance could be given that this was indeed the case. For this reason, results from single gauges were transformed into an equivalent normal stress acting in the model by direct multiplication of the indicated strain by the modulus of elasticity, and this resulting stress was then treated by Eqs. (1), (1a), or (2) as desired. It should be emphasized that this type of result does not give an accurate quantitative measure of stress at a given point, particularly shear stress, but that extremely high values of this quantity might be an indication of trouble which should be investigated in some detail.

QUANTITATIVE RESULTS

Quantitative results of the tests performed are given in the tables which follow as stresses in the prototype under the various conditions listed. Where shear stress is reported, it is the radius of the Mohr's circle of largest diameter which exists, as explained in the section on instrumentation, assuming that the stresses through the shell thickness are zero. For gauge locations, reference should be made to Westinghouse drawing 513F412, which has been coded at The University of Michigan and privately transmitted to the sponsor.

TABLE I

Final Stresses: S5W End-Plate Pressure Test

Stresses given are those which will exist in the prototype, as determined from test and the modeling laws.

Gauge or Gauges	Type	τ_{30},* psi	τ_{50},* psi	τ_{150},* psi
8, 9, 10	Rosette	424	706	2,120
13, 14, 15	Rosette	536	894	2,680
19, 22, 23	Rosette	357	595	1,785
27, 28, 29	Rosette	2522	4205	12,610
43, 44, 45	Rosette	652	1088	3,260
80, 81, 82	Rosette	1030	1720	5,150
91, 92, 93	Rosette	319	532	1,595
1, 2	90° pair	1096	1827	5,480
3, 4	90° pair	2160	3600	10,800
16, 17	90° pair	3340	5567	16,700
18, 30	90° pair	4150	6917	20,750
25, 26	90° pair	1215	2025	6,075
35, 36	90° pair	2550	4250	12,750
37, 38	90° pair	915	1525	4,575
39, 42	90° pair	3750	6250	18,750
40, 41	90° pair	2015	3360	10,075
47, 48	90° pair	1000	1667	5,000
49, 50	90° pair	2520	4200	12,600
51, 52	90° pair	1800	3000	9,000
53, 56	90° pair	692	1150	3,460
55, 57	90° pair	470	787	2,360
58, 64	90° pair	655	1090	3,275
65, 66	90° pair	885	1475	4,425
68, 69	90° pair	1060	1770	5,300
70, 71	90° pair	555	925	2,775
72, 95	90° pair	473	1715	2,365
74, 75	90° pair	535	890	2,675
83, 84	90° pair	560	930	2,800
85, 87	90° pair	440	730	2,200
89, 90	90° pair	550	920	2,750
94, 96	90° pair	935	1560	4,675
97, 98	90° pair	316	527	1,580
100, 101	90° pair	1675	2790	8,375
104, 105	90° pair	470	780	2,340

*Subscripts refer to the internal pressure in psi at which the above stresses will exist in the prototype.

TABLE I (concluded)

Gauge or Gauges	Type	σ_{30},* psi	σ_{50},* psi	σ_{150},* psi
5	Single gauge	-440	-730	-2,200
6	Single gauge	-895	-1490	-4,475
7	Single gauge	1140	1900	5,700
11	Single gauge	430	720	2,150
31	Single gauge	1170	1950	5,850
32	Single gauge	420	700	2,100
33	Single gauge	-1260	-2100	-6,300
34	Single gauge	770	1280	3,850
21	Single gauge	1010	1680	5,050
54	Single gauge	260	430	1,300
59	Single gauge	-730	-1220	-3,650
61	Single gauge	570	950	2,850
62	Single gauge	-810	-1350	-4,050
63	Single gauge	650	1080	3,250
67	Single gauge	640	1070	3,200
73	Single gauge	660	1100	3,300
76	Single gauge	790	1320	3,950
77	Single gauge	600	1000	3,000
78	Single gauge	400	670	2,000
79	Single gauge	-950	-1580	-4,750
86	Single gauge	690	1150	3,450
88	Single gauge	-720	-1200	-3,600
99	Single gauge	160	270	800
102	Single gauge	60	100	300
103	Single gauge	520	870	2,600

The results of the stress-coat tests have been discussed in the section on "Procedure" and have been presented in Figs. 7, 8, 9, and 10.

Numerical results from the transverse loading test are presented in Table II, based on a model load of 500 lb at each stub tube on the spacer plate, and treated with the modeling laws using 11,000 lb as the load on each actual stub tube in the prototype.

TABLE II

Final Stresses: S5W End-Plate Transverse Loading Test

Gauge or Gauges	Type	τ_{max}, psi	Gauge	Type	σ_{max}, psi
8, 9, 10	Rosette	4,840	5	Single	-2,120
13, 14, 15	Rosette	4,970	6	Single	-520
19, 22, 23	Rosette	8,990	7	Single	-2,610
27, 28, 29	Rosette	2,425	11	Single	3,770
44, 43, 45	Rosette	6,790	31	Single	10,400
80, 81, 82	Rosette	6,040	32	Single	-2,255
91, 92, 93	Rosette	10,100	33	Single	-9,130
1, 2	90° pair	2,330	34	Single	17,765
3, 4	90° pair	11,510	54	Single	2,170
16, 17	90° pair	13,887	59	Single	2,915
18, 30	90° pair	2,460	61	Single	20,050
25, 26	90° pair	2,600	62	Single	1,925
35, 36	90° pair	19,720	63	Single	8,770
37, 38	90° pair	3,675	67	Single	140
39, 42	90° pair	27,470	73	Single	-6,105
40, 41	90° pair	19,470	76	Single	-4,455
47, 48	90° pair	3,280	77	Single	935
49, 50	90° pair	6,140	78	Single	2,475
51, 52	90° pair	2,990	79	Single	-1,980
53, 56	90° pair	600	86	Single	-800
55, 57	90° pair	1,650	88	Single	-4,760
58, 64	90° pair	1,060	99	Single	-850
65, 66	90° pair	835	102	Single	11,030
68, 69	90° pair	21,560	103	Single	3,440
70, 71	90° pair	4,650	106	Single	14,300
72, 95	90° pair	5,210	107	Single	770
74, 75	90° pair	8,630	108	Single	26,370
83, 84	90° pair	3,680	109	Single	63,060
85, 87	90° pair	6,890	110	Single	35,340
89, 90	90° pair	4,010	111	Single	30,770
94, 96	90° pair	8,476	112	Single	3,160
97, 98	90° pair	5,970	113	Single	-1,925
100, 101	90° pair	4,620	114	Single	-1,350
104, 105	90° pair	6,500	115	Single	4,540
			21	Single	-715

Results from the axial loading tests are given in Table III in terms of stresses in the prototype. These tests were run at a model load of 1000 lb at each stub tube, and assuming a prototype dead weight of each module equal to 348 lb.

TABLE III

Final Stresses: S5W End-Plate Axial Loads

Gauges	Type	τ_{max}, psi	Gauge	Type	σ_{max}, psi
8, 9, 10	Rosette	366	5	Single	392
13, 14, 15	Rosette	376	6	Single	413
19, 22, 23	Rosette	353	7	Single	338
27, 28, 29	Rosette	767	11	Single	413
43, 44, 45	Rosette	293	31	Single	243
80, 81, 82	Rosette	479	32	Single	89
91, 92, 93	Rosette	167	33	Single	594
1, 2	90° pair	276	34	Single	502
3, 4	90° pair	1016	54	Single	96
16, 17	90° pair	1000	59	Single	139
18, 30	90° pair	1163	61	Single	83
25, 26	90° pair	493	62	Single	47
35, 36	90° pair	747	63	Single	135
37, 38	90° pair	278	67	Single	163
39, 42	90° pair	1170	73	Single	223
40, 41	90° pair	1074	76	Single	227
47, 48	90° pair	366	77	Single	145
49, 50	90° pair	1204	78	Single	246
51, 52	90° pair	131	79	Single	432
53, 56	90° pair	186	86	Single	91
55, 57	90° pair	209	88	Single	174
58, 64	90° pair	268	99	Single	53
65, 66	90° pair	323	102	Single	77
68, 69	90° pair	278	103	Single	571
70, 71	90° pair	239	106	Single	956
72, 95	90° pair	119	107	Single	684
74, 75	90° pair	294	108	Single	920
83, 84	90° pair	289	109	Single	2383
85, 87	90° pair	128	110	Single	1396
89, 90	90° pair	330	111	Single	2207
94, 96	90° pair	303	112	Single	306
97, 98	90° pair	144	113	Single	319
100, 101	90° pair	99	114	Single	468
104, 105	90° pair	93	115	Single	527
			21	Single	420

Due to a lack of space in the bed of the testing machine, it was not possible to load each of the stub tubes separately. However, the central tube, when loaded separately, showed a maximum strain in gauges 85-87, which resulted

in an actual shear stress in the model of 1175 psi, and treating this with Eq. (2), the largest concentrated load which can be carried by the central stub tube, based on a prototype allowable stress of 10,250 psi, is

$$P_{max} = \frac{4000}{1175}(10{,}250) = 34{,}900 \text{ lb} .$$

The deflection of the spacer plate with respect to the shell was measured separately by a dial gauge mounted between the shell and spacer plate, and was taken for transverse loads only. Using model loads of 1000 lb per stub tube, the prototype spacer-plate deflection is given by

$$\delta_p = \delta_m \cdot \frac{L_p}{L_m} \cdot \frac{a_m}{a_p} \frac{E_m}{E_p} , \qquad (5)$$

where

δ = deflection,
a = scale,
E = modulus of elasticity,
L = load,

and where the subscripts m and p refer to the model and prototype, respectively. Using a modulus of 10 x 10^6 psi for aluminum, and 25.5 x 10^6 psi for steel, a scale factor of $a_m/a_p = 1/2$, and using the measured model deflection of .515 in., the deflection of the prototype is

$$\delta_p = .103 \text{ in.}$$

Finally, since gauges 39, 42, 109, and 110 showed rather high strain readings, rosettes were constructed of Type A-18 gauges and attached at these points. The reduced maximum shear stresses in the prototype obtained from these rosettes are given in Table IV for the case of transverse loading of the modules only.

TABLE IV

Prototype Shear Stresses due to Transverse Loads, from Rosette Data

Area of Gauge Attachment	τ_{max}, psi
39, 42 (117)	19,740
109 (118, 119)	31,110
110 (120, 121)	18,250
111 (122, 123)	18,250

The gauge numbers listed in parentheses in Table IV are gauges added to make rosettes in conjunction with the gauges already present.

APPENDIX

COMPARISON OF EXPERIMENT WITH ANALYSIS

A review of the analysis was made to pick out those calculated stresses which could be compared directly to measured stresses. Table AI given below indicates those comparisons where warranted. Position of the existing stress is indicated by the gauge position noted in the table, in terms of the gauge number.

TABLE AI

Gauge or Gauges	Measured Stress, psi	Calculated Stress, psi	Vol. I[2] Part	Vol. I[2] Page
	Transverse Loading			
61	σ = 20,050	σ = 2,670	2	6
70,71	τ = 4,650	τ = 1,850	2	6
75	σ = -9,250	σ = 9,200	3	7
68,69	τ = 21,650	τ = 32,800	3	11
		τ = 14,500	3	11
91,92,93	τ = 10,100	τ = 19,600	3	13
72,95	τ = 5,210			
53,56	τ = 600			
58,64	τ = 1,060			
85,87	τ = 6,890			
5	$\tau = \sigma/2 = -2120/2 = -1060$			
7	$\tau = \sigma/2 = -2610/2 = -1305$	τ = 3,240	4	13
59	$\tau = \sigma/2 = 2915/2 = 1457$			
73	σ = -6,105	σ = 6,060	4	13

TABLE AI (continued)

Gauge or Gauges	Measured Stress, psi	Calculated Stress, psi	Vol. I[2] Part	Page
104,105	τ = 6,500	τ = 9,560	5	5
39,42	τ = 27,470			
37,38	τ = 3,675			
94,96	τ = 8,476			
16,17	τ = 13,887			
65,66	τ = 835			
18,30	τ = 2,460			
25,26	τ = 2,600			
31	σ = 10,400	σ = 2,020	6	6
78	σ = 2,475			
16,17	τ = 13,887	τ = 2,260	6	6
65,66	τ = 835			
18,30	σ = -1,400	σ = -4,260	6	6
43,44,45	τ = 6,790	τ = 4,590	6	10
16,17	τ = 13,887	τ = 27,000	6	12
65,66	τ = 835	τ = 14,200	6	14
18,30	τ = 2,460			
25,26	τ = 2,600			
35,36	τ = 19,720			
89,90	τ = 4,010			
1,2	τ = 2,330	τ = 3,270	7	5
51,52	τ = 2,990	τ = 3,060	7	5
100,101	τ = 4,620			
47,48	τ = 3,280			
3,4	τ = 11,510	τ = 1,960	7	6
49,50	τ = 6,140			
	Axial Loads		Vol. II[2]	
3,4	τ = 1,016	τ = 563	2	3
49,50	τ = 1,204			
40,41	τ = 1,074			

TABLE AI (concluded)

Gauge or Gauges	Measured Stress, psi	Calculated Stress, psi	Vol. II[2] Part	Page
		Pressure Loads		
3,4	τ = 2,160	τ = 8,040	4	4
49,50	τ = 2,520			
40,41	τ = 2,015			
1,2	τ = 1,096	τ = 2,600	4	5
51,52	τ = 1,800			
47,48	τ = 1,000			
100,101	τ = 1,675			
	Deflections: Transverse Loading Spacer Plate with Respect to Shell			
	δ = .103 in.	δ = .002 in.	4	12

Fig. 1. Shell, switch boxes, and bridge in place for pressure test.

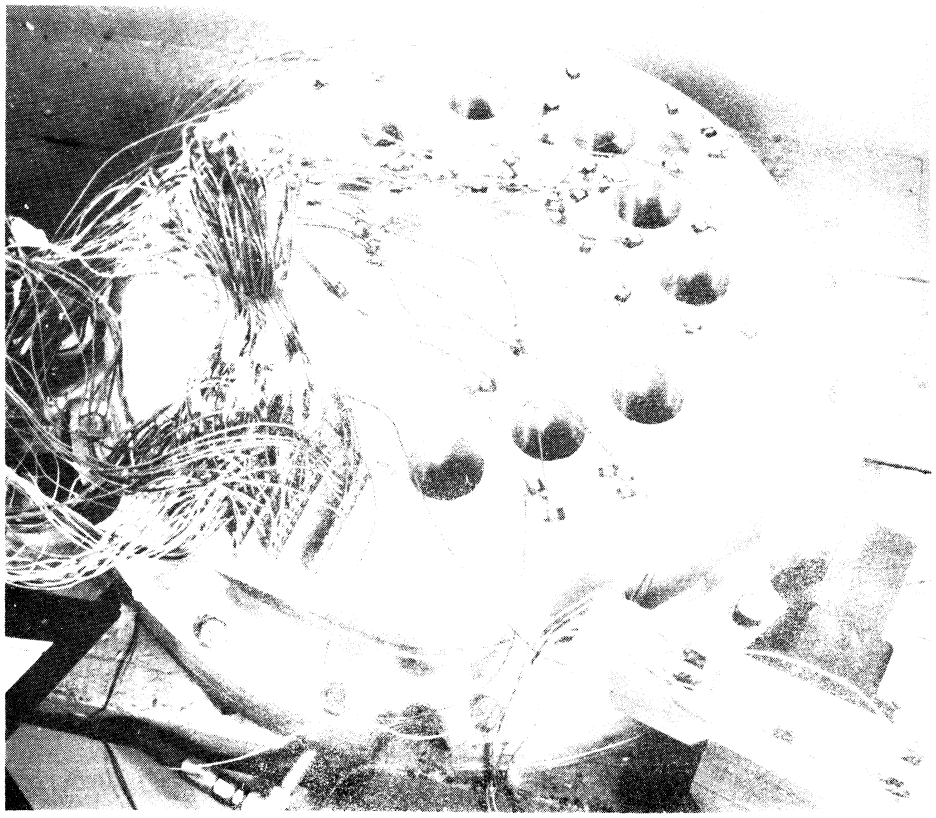

Fig. 2. Close-up of shell showing gauge wiring.

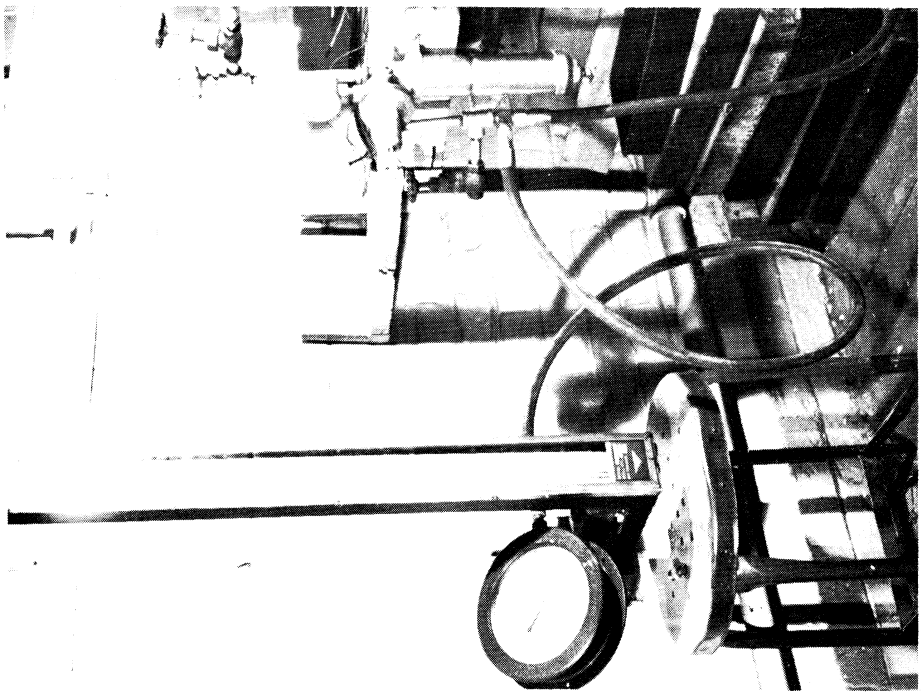

Fig. 4. Manometer, pressure gauge, and relief valve used in pressure tests.

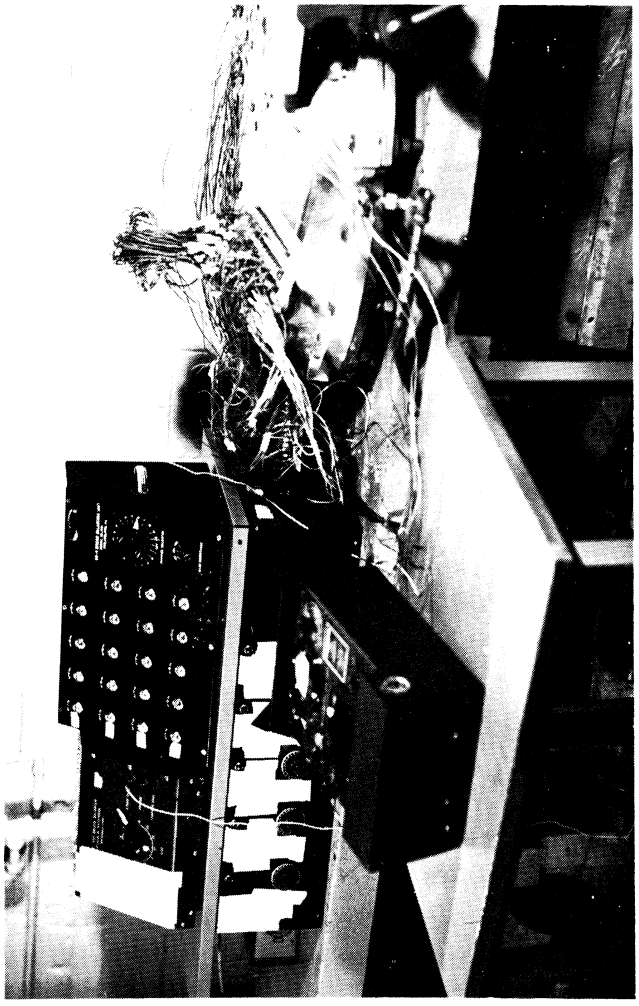

Fig. 3. General test arrangement for pressure loading.

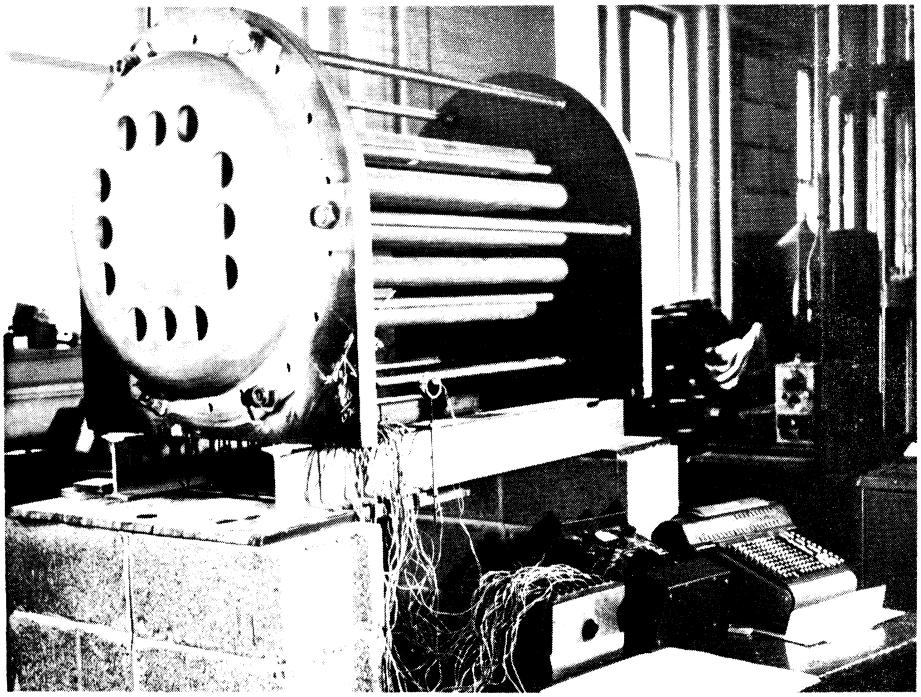

Fig. 5. General test arrangement for transverse loading of plexiglass shell.

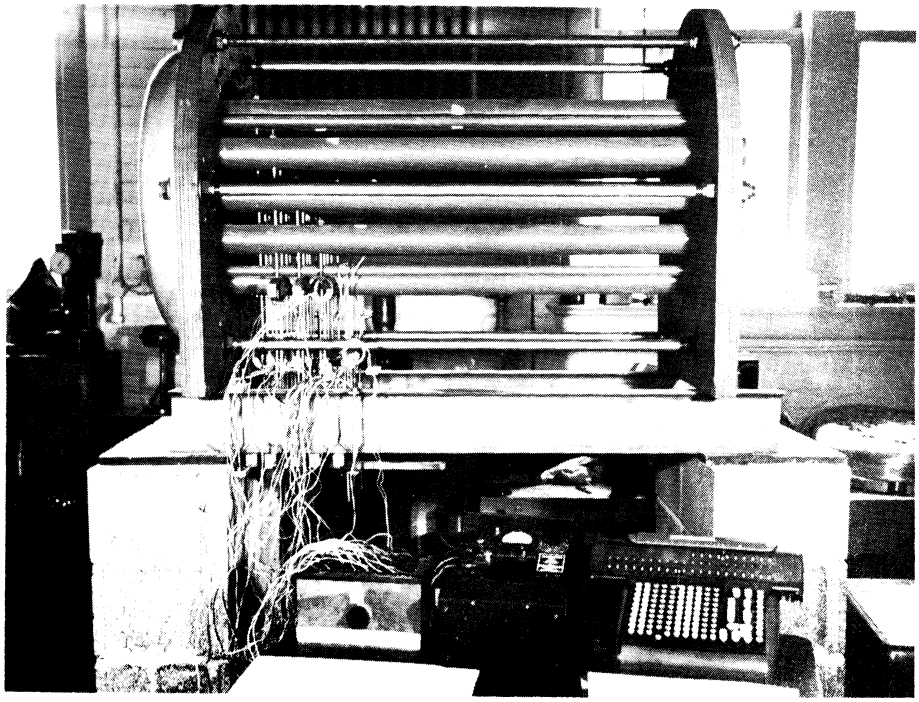

Fig. 6. Test arrangement for loading of plexiglass shell showing ring dynamometers.

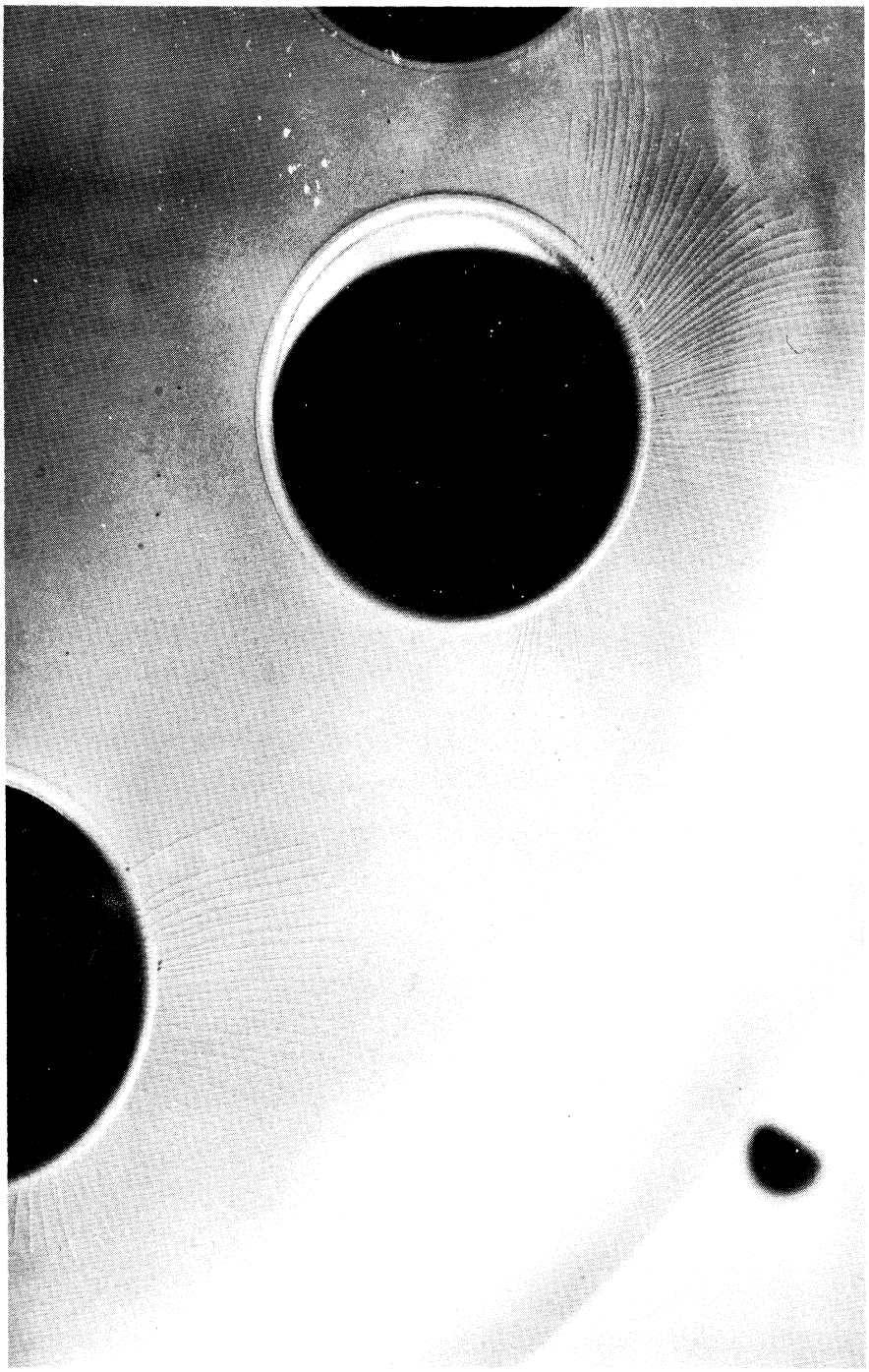

Fig. 7. Stress-coat cracks in plexiglass shell with transverse loading.

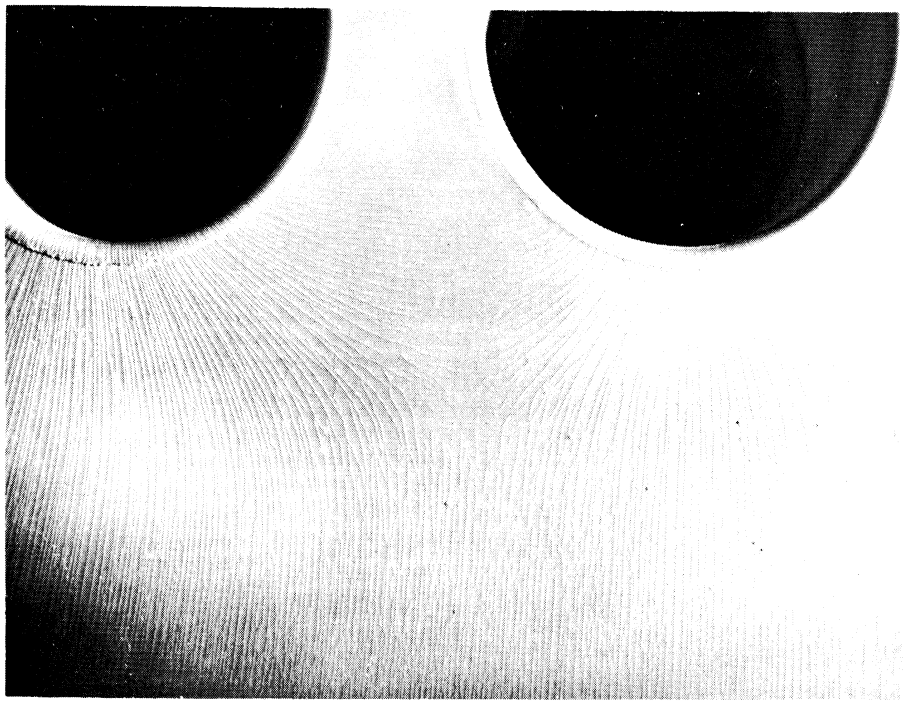

Fig. 8. Stress-coat cracks in plexiglass shell after sensitization.

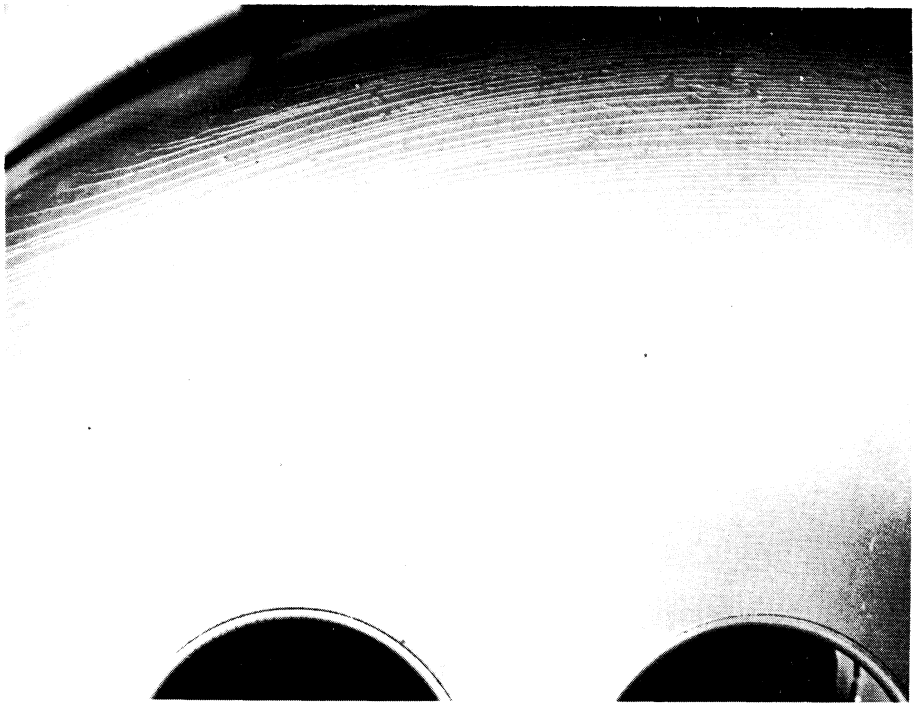

Fig. 9. Stress-coat cracks in plexiglass shell in the region of the toroidal section, after sensitization.

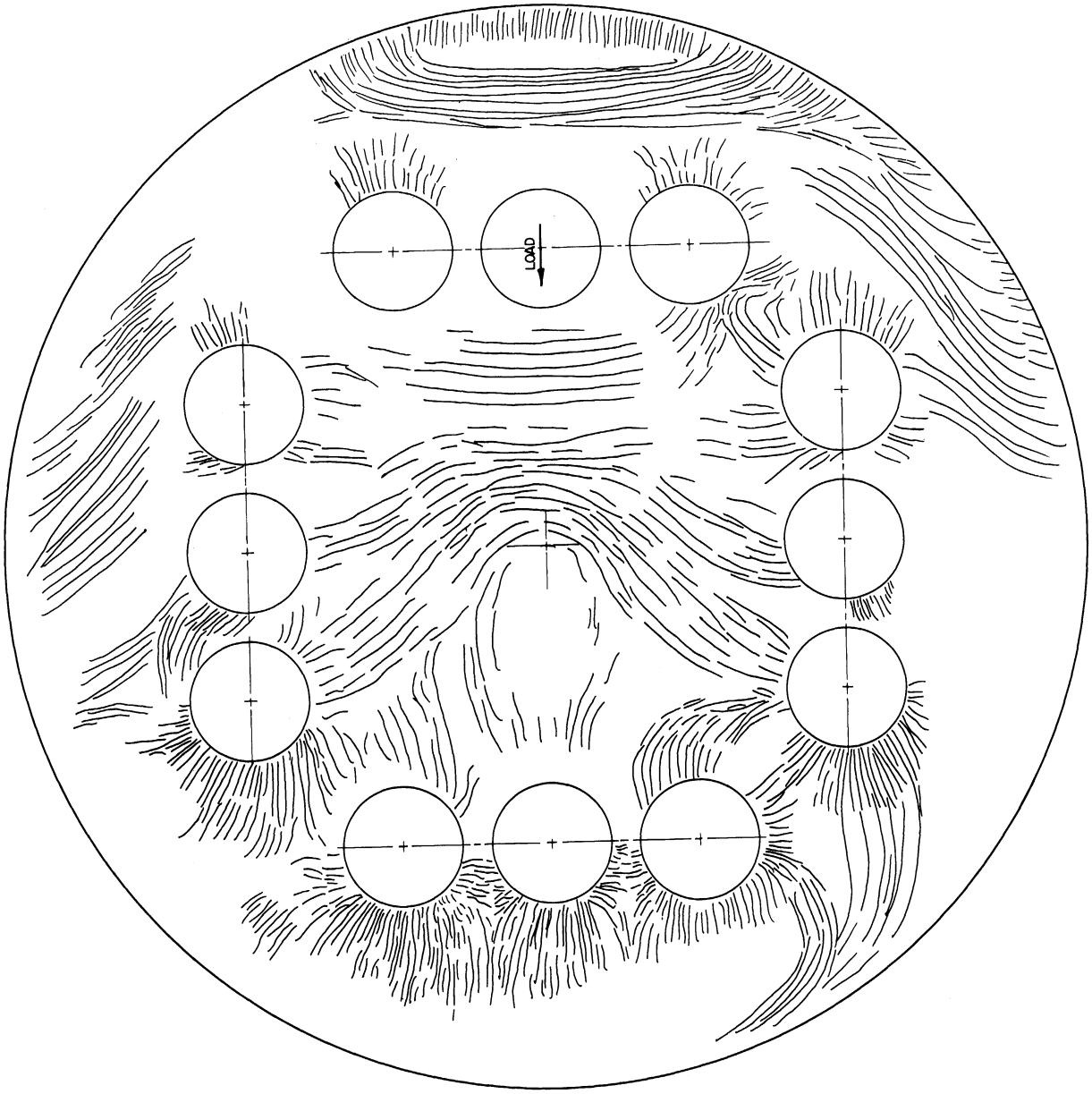

TOP VIEW

Fig. 10. Overall stress-coat crack pattern on plexiglass model under transverse loading.

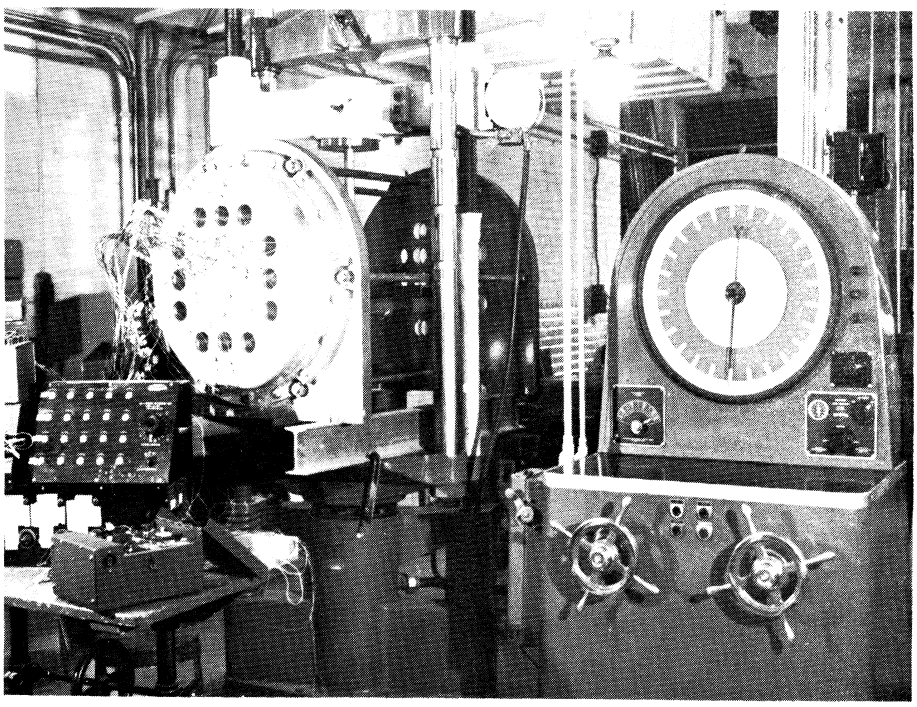

Fig. 11. General test arrangement for transverse loading of aluminum shell.

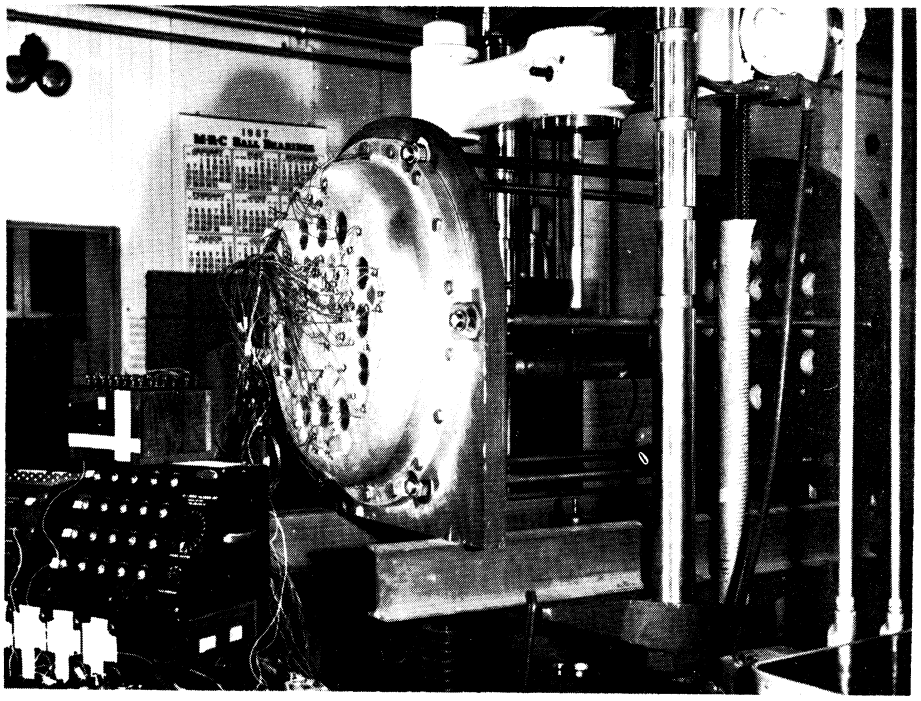

Fig. 12. Transverse loading of aluminum shell showing method of load application.

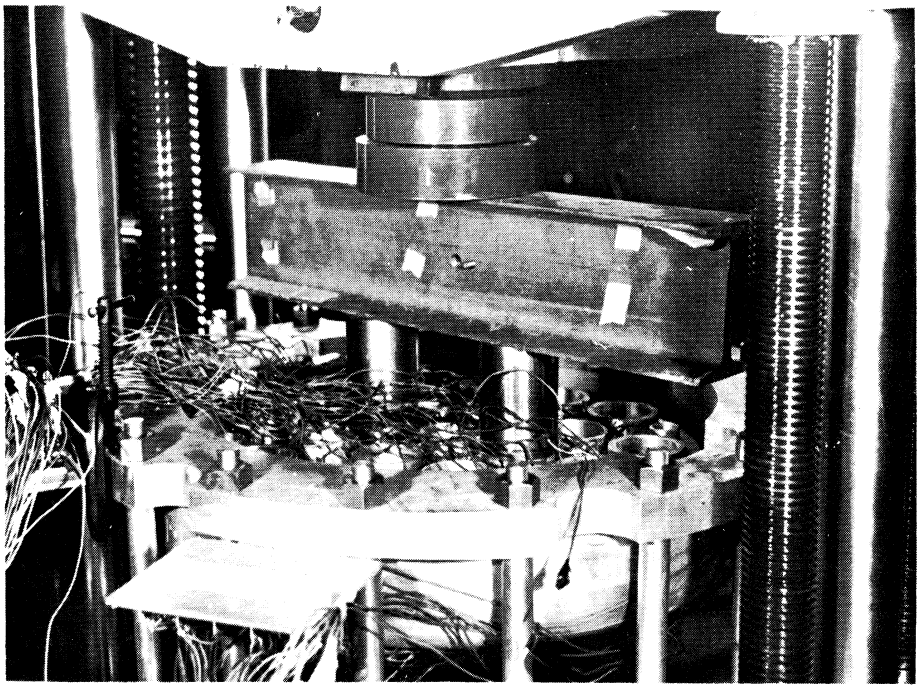

Fig. 13. General test arrangement for axial loading of aluminum shell.

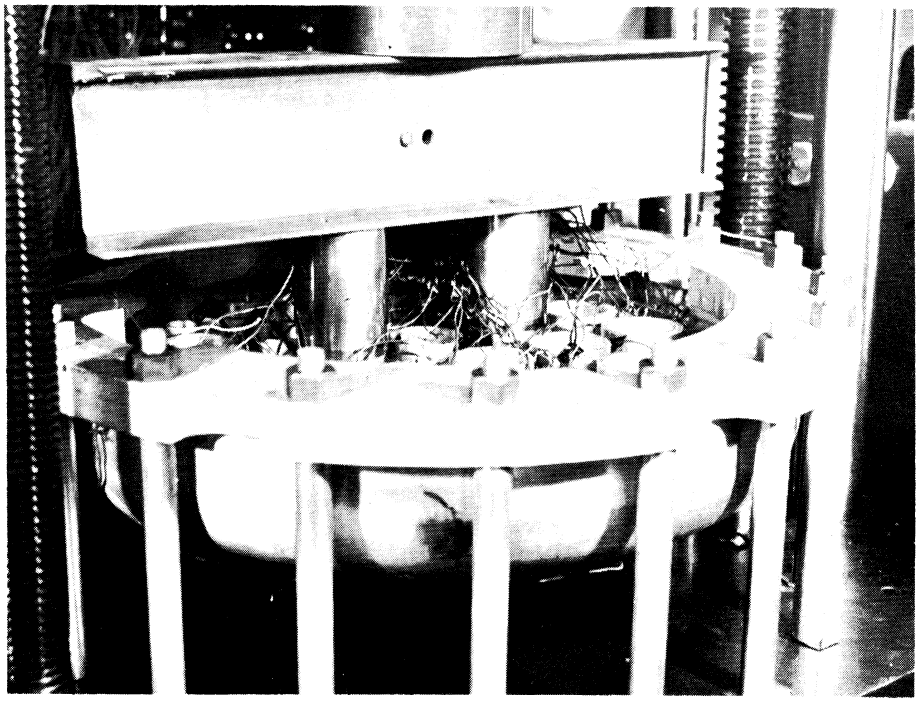

Fig. 14. Axial loading of aluminum shell showing supporting legs bearing on flat bedplate of testing machine.

REFERENCES

1. Hetényi, M., Handbook of Experimental Stress Analysis, John Wiley and Sons, New York, 1950.

2. Rowley, J. C., Unpublished analysis of bottom-plate structure of the S5W reactor barrel, August, 1956. Transmitted privately to Westinghouse Electric Corporation.